Pten coordinates retinal neurogenesis by regulating Notch signalling

Hong Seok Jo[1], Kyung Hwa Kang[2], Cheol O Joe[1,2] and Jin Woo Kim[1,2,*]

[1]Department of Biological Sciences, Korea Advanced Institute of Science and Technology (KAIST), Daejeon, Republic of Korea and [2]Institute of BioCentury, Korea Advanced Institute of Science and Technology (KAIST), Daejeon, Republic of Korea

Development of nervous tissue is a coordinated process of neural progenitor cell (NPC) proliferation and neuronal differentiation. Intracellular signalling events that regulate the balance between NPC proliferation and neuronal differentiation, therefore, determine the size and composition of nervous tissues. Here, we demonstrate that negative regulation of phosphoinosite 3-kinase (PI3K)-Akt signalling by phosphatase tensin homologue (Pten) is essential for maintaining NPC population in mouse retina. We found that mouse retinal progenitor cells (RPCs) lacking the *Pten* gene complete neurogenesis earlier than their normal developmental schedule, resulting in their premature depletion in the mature retina. We further discover that Notch intracellular domain (NICD) fails to form transcription activator complex in *Pten*-deficient RPCs, and thereby unable to support RPC maintenance. Taken together, our results suggest that Pten plays a pivotal role in retinal neurogenesis by supporting Notch-driven RPC maintenance against neurogenic PI3K-Akt signalling.

Introduction

The generation of neurons that compose vertebrate nervous system is accomplished by the repeated division of neural progenitor cells (NPCs; reviewed in Gotz and Huttner, 2005). NPC division gives rise to daughter cells that either retain NPC characteristics or differentiate into specific types of neurons (reviewed in Gotz and Huttner, 2005 and Zhong and Chia, 2008). Although the fates of NPC-derived cells increasingly diverge with successive cell divisions, the neuronal subsets in a given species are well conserved at both final and intermediate stages (Cepko *et al*, 1996; Edlund and Jessell, 1999; Livesey and Cepko, 2001; Cayouette *et al*,

*Corresponding author. Department of Biological Sciences, Korea Advanced Institute of Science and Technology (KAIST), 291 Daehak-ro, Yuseong-gu, Daejeon 305-701, Republic of Korea.
Tel.: +82 42 350 2641; Fax: +82 42 350 2610;
E-mail: jinwookim@kaist.ac.kr

2003). This predictable feature of neural development has been explained by the existence of genetic programs that operate in a spatial- and temporal-specific manner to accurately control neuronal differentiation.

The mouse retina has been exploited as a model to investigate mammalian neurogenic programs. Using this model, it has been shown that six types of retinal neurons and Müller glia (MG) are generated in an ordered manner during development (Cepko *et al*, 1996; Harris, 1997). It has been also suggested that the sequential production of retinal cells is mediated by serial changes in the competence of retinal progenitor cells (RPCs) over developmental time (Cepko *et al*, 1996; Harris, 1997; Livesey and Cepko, 2001; Raff, 2006). Two hypotheses, which are not mutually exclusive, have been proposed to explain the transition in RPC competence. One emphasizes intrinsic control by genetic programs, and the other suggests that this transition is mainly influenced by changes in the local environment (Turner *et al*, 1990; Cepko *et al*, 1996; Cayouette *et al*, 2003). The former argues that each RPC is predestined to generate specified types of retinal cells regardless of external conditions (Cayouette *et al*, 2003), whereas the latter predicts that a single retinal cell type would be produced predominantly from RPCs if the environment remained constant (Livesey and Cepko, 2001). A unified concept, which combines elements of both hypotheses, proposes that the developmental transition is governed by reciprocal interactions between intrinsic developmental programs and the local cellular environment (Cepko *et al*, 1996; Livesey and Cepko, 2001). For instance, extracellular factors produced by previously generated retinal neurons through the operation of intrinsic developmental programs could act as environmental factors to affect subsequently dividing RPCs (Wang *et al*, 2002; Kim *et al*, 2005; Liu *et al*, 2007). The factors not only mean secreted factors, such as RGC-produced growth and differentiation factor 11 (GDF11), which promotes the differentiation of mouse RPCs into retinal neurons (Kim *et al*, 2005), and Wnts, which are secreted from ciliary margin or retinal pigment epithelium (RPE) to facilitate RPC proliferation (Cho and Cepko, 2006; Liu *et al*, 2007), but also include cell–cell contact-dependent signalling mediated by Notch, which supports RPC or glial fate (Furukawa *et al*, 2000; Jadhav *et al*, 2006; Yaron *et al*, 2006). However, multiple developmental signals might act simultaneously on RPCs to trigger distinct and specific intracellular signalling cascades to induce expression of unique target gene sets (Livesey and Cepko, 2001; Lamba *et al*, 2008; Agathocleous and Harris, 2009). Owing to this inherent complexity, it remains difficult to predict the final responses of RPCs to individual inputs.

In contrast to the complexity of input signals, responses of RPCs could be generalized, either through maintenance of progenitor characteristics that allow cells to re-enter the cell cycle or through differentiation into specific types of neurons after exiting from the cell cycle (Lamba *et al*, 2008; Agathocleous and Harris, 2009). We, therefore, hypothesized

that concomitantly acting external signals merge at common intracellular signalling hubs, the activities of which determine the relative dominance of RPC maintenance versus neuronal differentiation. A number of ubiquitously distributed intracellular signalling pathways, including cyclic AMP (cAMP)/protein kinase A (PKA), phosphoinositide-3 kinase (PI3K)-Akt, phospholipase C (PLC)-protein kinase C (PKC), and mitogen-activated protein kinase (MAPK) signalling pathways, have been proposed to act as feasible intracellular signalling hubs for multiple developmental cues on the basis of their ability to respond to multiple external factors and control cell proliferation and differentiation (Cantley, 2002; Stork and Schmitt, 2002; Engelman et al, 2006; Hui et al, 2007; Raman et al, 2007; Chiaradonna et al, 2008; Gould and Newton, 2008).

The PI3K-Akt signalling pathway has been shown to integrate multiple developmental signals, including sonic hedgehog (Shh), Wnt, fibroblast growth factor (FGF), and insulin-like growth factor (IGF) (Fischer et al, 2002; Peng et al, 2004; Fischer, 2005; Riobo et al, 2006; Peltier et al, 2007; Wolf et al, 2008) in various cell types, and thereby support cell growth, proliferation, and survival. Interestingly, PI3K-Akt signalling activity is strongly enriched in post-mitotic retinal neurons than in RPCs. This intriguing observation prompted us to investigate the regulatory role of the PI3K-Akt signalling pathway in retinal neurogenesis, using mice in which the phosphatase tensin homologue (Pten) gene is specifically eliminated from developing RPCs. The resulting absence of Pten, which negatively regulates Akt, leads to constitutive activation of Akt in these cells. Pten-deficient RPCs hyperproliferated during development, but were prematurely depleted in the mature retina. Neurogenesis from Pten-deficient RPCs was enhanced, leading to earlier completion of retinal development than normal schedule. We found that the activity of the Notch signalling pathway was decreased in the Pten-cko retina due to inhibition of the Notch transcription complex formation. Collectively, our results show that Pten regulation of PI3K-Akt signalling is a critical component of the intracellular signalling that coordinates retinal neurogenesis and RPC maintenance.

Results

Specific enrichment of Akt activity in post-mitotic retinal neurons

To delineate intracellular signalling pathways that might serve as key determinants of the relative dominance of RPC maintenance versus neuronal differentiation in mouse retinas, we examined the activities of various intracellular signalling pathways by immunostaining with phospho-specific antibodies that recognize the active form of the corresponding signalling components (data not shown). These preliminary experiments revealed that the immunofluorescence signal for active PI3K-Akt signalling pathway, examined using an anti-phospho-Akt[S473] (pAkt) antibody (Alessi et al, 1996), was inversely correlated with RPC-specific Chx10 expression (Chen and Cepko, 2000) and closely overlapped with the expression of post-mitotic neuron-specific Islet1 (Elshatory et al, 2007; Figure 1A). These results suggest a potential role for PI3K-Akt signalling in the neuronal differentiation of RPCs.

Robust expansion of Pten-deficient cell population in Pten-cko retina

We, therefore, investigated the role of the PI3K-Akt signalling pathway in RPCs by modulating its activity in vivo. Pten, which encodes a major cellular phosphoinositide 3-phosphatase that opposes PI3K activity (reviewed in Salmena et al, 2008), is broadly expressed in developing and adult mouse retina (Kim et al, 2008), and it regulates regeneration of RGC axons (Park et al, 2008) and structural integrity of RPE (Kim et al, 2008). However, the roles of Pten in developing mouse retina have not been assessed.

The Pten gene was specifically deleted in RPCs by crossing Pten-flox mice (Suzuki et al, 2001) with Pax6 α-Cre (Pax6-aCre) mice (Marquardt et al, 2001), in which expression of Cre recombinase and internal ribosome entry site (IRES)-linked enhanced green fluorescent protein (EGFP) is driven by the Pax6 α-enhancer in the distal RPC population (Figure 1B). We then obtained Pten^{flox/flox};Pax6-aCre (Pten-cko) mice that are predicted to maintain constitutively increased Akt activity specifically in Pax6 α-enhancer-positive distal RPCs and their derivative retinal cell lineages. As expected, Pten was eliminated in E14.5Pax6-aEGFP-positive distal RPCs (Figure 1C, upper row; split colour channel images are shown in Supplementary Figure S1); and consequently, pAkt level was elevated in the area (Figure 1C, bottom row).

We anticipated that this manipulation would allow us to compare the developmental patterns of the genetically modified distal area with that in unaffected proximal areas of the same retina. However, Pten-deficient cells were not simply restricted to the distal retina of Pten-cko mice. Using the Cre recombinase-sensitive ROSA26-lacZ reporter (R26-lacZ; Soriano, 1999) to indirectly trace cells that had undergone Cre-mediated deletion of Pten, we found that the R26-lacZ-positive region in the E14.5 Pten-cko retina extended into the proximal region, a presumed Pax6 α-enhancer-negative region (Figure 1D). This unexpected proximal expansion of Pten-deficient cells was more evident in the postnatal day 4 (P4) retina, which was entirely R26-lacZ positive and Pten deficient (Supplementary Figure S2).

Premature depletion of hyperproliferating Pten-deficient RPCs

The increase in Pten-deficient cells in the Pten-cko retinas might have resulted from either hyperproliferation or enhanced cell survival, both of which are strongly supported by PI3K-Akt signalling pathway (reviewed in Cantley, 2002; Engelman et al, 2006 and Salmena et al, 2008). There were indeed fewer apoptotic (TUNEL positive) cells among the P5 Pten-deficient retinal cells, which were R26-lacZ positive, than among the R26-lacZ-negative normal retinal cells (Supplementary Figure S3). These results indicate that the predominance of Pten-deficient retinal cells in the postnatal Pten-cko retina might be a reflection of their enhanced survival or their non-autonomous induction of cell death in neighbouring wild-type retinal cells.

We also found that there were more proliferating retinal cells in embryonic and neonatal Pten-cko retinas than in the retinas of corresponding wild-type littermates, as detected by incorporation of the thymidine analogue, bromodeoxyuridine (BrdU) (Figure 2A, upper row; Figure 2B) or by counting phospho-histone H3 (pH3)-positive mitotic cells (Supplementary Figure S4). Pulse-chase labelling with other thymidine
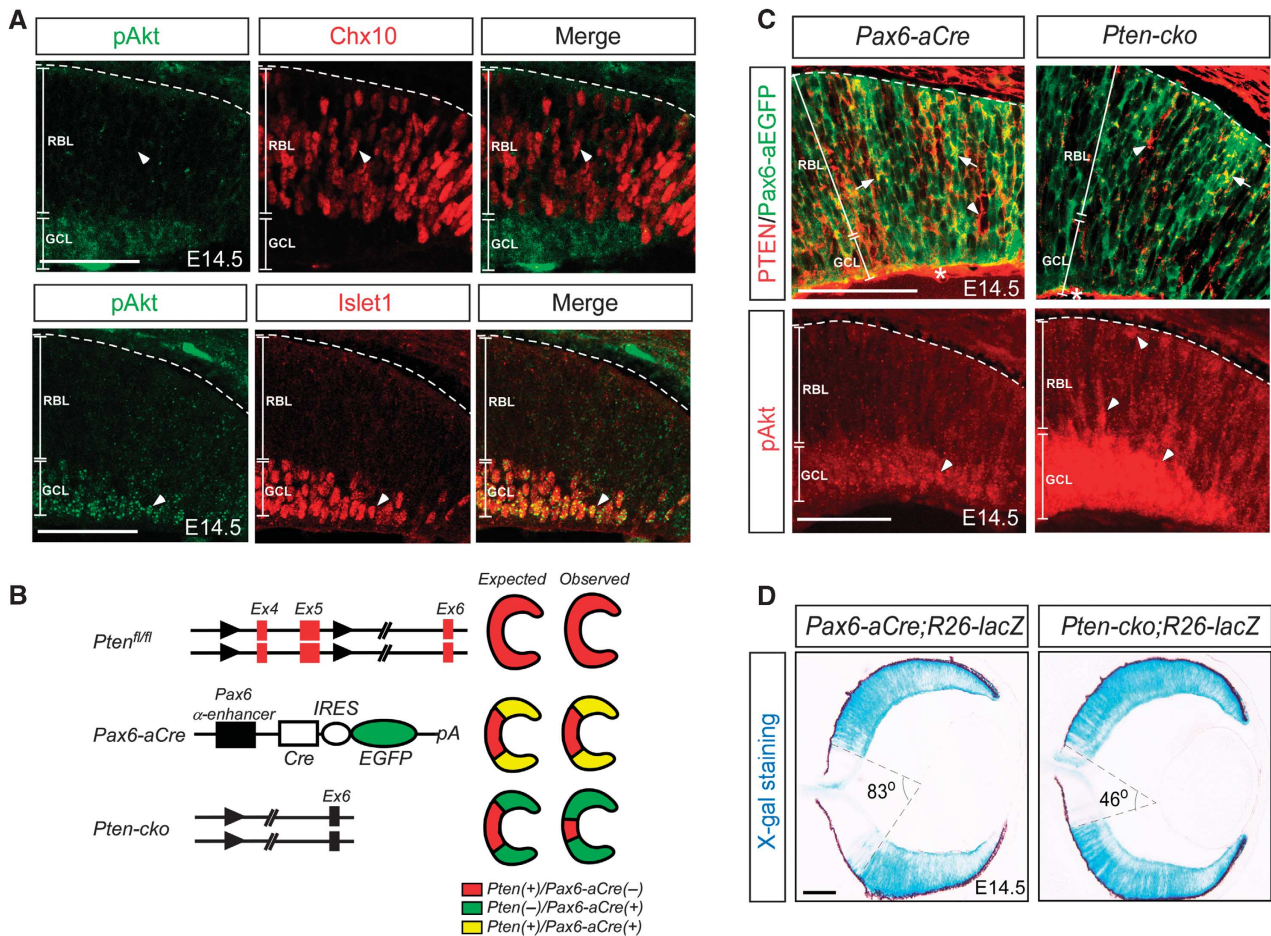
Figure 1 Specific enrichment of Akt activity in post-mitotic retinal neurons. (**A**) The activity of PI3K-Akt signalling in the developing mouse retina was examined by co-immunostaining using a rabbit anti-phospho-Akt[S473] antibody (pAkt; green) that recognizes activated Akt, and guinea pig antibodies that detect Chx10 expression in RPCs (red in top row) or Islet1 in post-mitotic neurons (red in bottom row). Arrowheads indicate Chx10-positive RPCs that lack pAkt (top row) and Islet1-positive post-mitotic neurons that co-express pAkt (bottom row), respectively. (**B**) Schematic diagram for spatial-specific elimination of *Pten* gene (red) in mouse retina using *Pten-flox* and *Pax6-aCre* (green) mice (Marquardt *et al*, 2001; Suzuki *et al*, 2001). (**C**) Corresponding to the *Pten* elimination, pAkt level was significantly increased in *Pten-cko* mouse retina. Arrows and arrowheads at top row indicate Pten(+)/EGFP(−) and Pten(+)/EGFP(+) cells, respectively. Arrowheads at bottom row indicate pAkt-positive cells. *Pten expressed in extra-retinal cells. (**D**) Distribution of *Pten*-deficient cells in E14.5 *Pten-cko* mouse retina was indirectly examined by X-gal staining (blue) that detects β-galactosidase expressed by R26-lacZ reporter (R26-lacZ) gene cassette upon the Pax6-aCre-dependent recombination. The area that was unaffected by the Pax6-aCre-dependent recombination (X-gal-negative inside area of the cone) was reduced to 46° angle in E14.5 *Pten-cko;R26R* retina from 83° angle at the equivalent position of littermate *Pax6-aCre;R26R* retina. RBL, retinoblast layer; GCL, ganglion cell layer. Scale bars in the pictures represent 50 μm. Dashed lines in the pictures represent retina-RPE borders.

analogues, chlorodeoxyuridine (CIdU), and iododeoxyuridine (IdU), further indicated that, on average, the cell-cycle period of cells in *Pten-cko* embryonic retinas was also shorter (Supplementary Figure S5). Faster accumulation of *Pten*-deficient cells compared with wild-type cells, resulting from a combination of shortened RPC cell-cycle period and increased number of dividing RPCs, therefore likely caused the proximal expansion of *Pten*-deficient cells in the *Pten-cko* retina.

However, by P4, the number of BrdU-positive proliferating cells in *Pten-cko* retinas had rapidly decreased to a level even less that in the retinas of *Pax6-aCre* littermates (Figure 2A, bottom row; Figure 2B). The number of Sox2-positive RPCs in *Pten-cko* retinas at this stage was also significantly reduced (Figure 2C and D). Mutant retinas did not show a subsequent recovery in the number of proliferating cells. Thus, these results indicate that *Pten*-deficient RPCs hyperproliferated during development, but prematurely lost their potential to

generate retinal cells during the postnatal period. The loss of postnatal RPCs in *Pten-cko* mice often led to retinal degeneration, which was observed in ~28% of adult *Pten-cko* mice (data not shown).

Reduced MG numbers in Pten-cko retinas

The neurogenic schedule in the mouse retina is well defined, with specific retinal cell types being predominantly generated during delimited developmental periods (Livesey and Cepko, 2001). Therefore, the dramatic change in proliferation potential of *Pten*-deficient RPCs during development might influence the composition of the retina through a gain in early-born retinal cells, such as retinal ganglion cells (RGCs), amacrine cells (ACs), horizontal cells (HZs), cone photoreceptors (cPRs), and rod photoreceptors (rPRs), and/or loss of late-born retinal cells, such as bipolar cells (BPs) and Müller glial cells (MGs). To address this possibility, we examined the distribution of retinal cells in *Pax6-aCre* and *Pten-cko* retinas
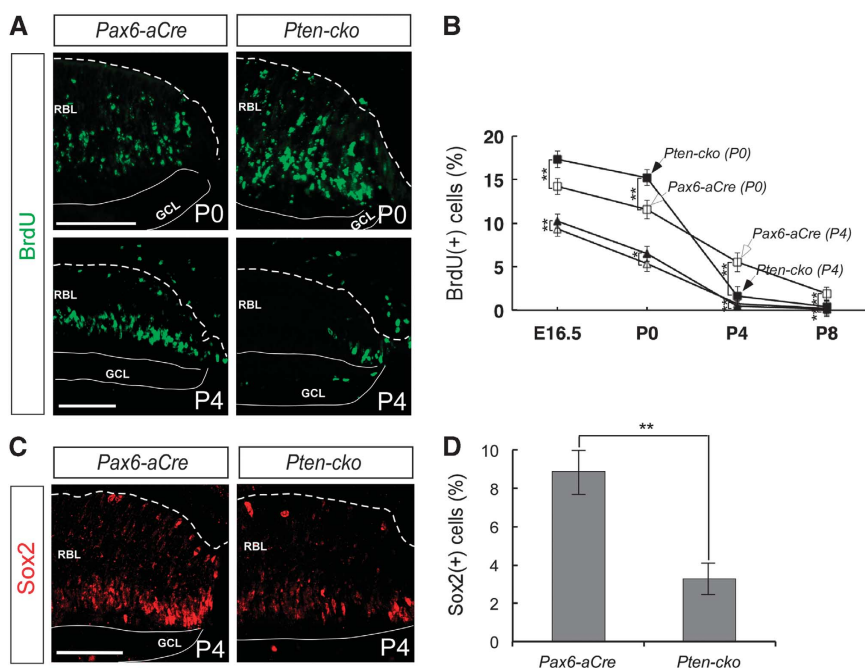
Figure 2 Premature depletion of hyperproliferating *Pten*-deficient RPCs. (**A**) The proliferating cells in P0 and P4 retinas were detected by immunostaining with an anti-BrdU antibody (see details in Materials and methods). (**B**) The BrdU-positive cells in the proximal and distal retina at distinct developmental stages were counted. The open squares and open triangles indicate percentage of BrdU-positive cells in distal and proximal areas of the *Pax6-aCre* retina, respectively, whereas the closed squares and solid triangles indicate percentage of BrdU-positive cells in the distal and proximal areas of the *Pten-cko* retina. *Y* axis values in the graph are the mean value obtained from six (E16.5 and P0 samples) or eight (P4 and P8 samples) different samples taken of retinal sections isolated from three (E16.5 and P0 samples) or four (P4 and P8 samples) independent litters. Error bars denote standard deviation (s.d.). *P-value < 0.01; **P-value < 0.005. (**C**) The distribution of Sox2-positive RPCs in P4 mouse retinas was examined by immunostaining with an anti-Sox2 antibody. (**D**) The mean values of Sox2-positive RPCs, obtained from data of six different images of eye sections from three independent litters, are displayed. Error bars denote s.d. **P-value < 0.005. Scale bars in (**A**) and (**C**) indicate 50 μm. Dashed lines in the pictures represent retina-RPE borders.

at P8, a time when most retinal cell types have already been generated but they have not started daily visual activity yet. The numbers of early-born cells, including RGCs, ACs, and HZs, as well as the number of late-born BPs in *Pten-cko* retinas were not significantly different from those in *Pax6-aCre* retinas (Figure 3A–H and M). In contrast, the number of MGs in *Pten-cko* retinas was reduced by ∼33% compared with that in *Pax6-aCre* retinas, and there was a complementary increase of ∼27% in the number of PRs (Figure 3I–M). However, the increased PR numbers were not be able to persist until adult *Pten-cko* retinas, of which PRs were decreased about 17% of *Pax6-aCre* or *Pten-flox* littermates' retinas (data not shown).

Accelerated development of Pten-cko retinas
In contrast to the unchanged final composition of retinal neurons, except for the reduced MG cell numbers, in *Pten-cko* mice, the numbers of retinal neurons in developing *Pten-cko* mice were higher than those of littermate *Pax6aCre* mice. The numbers of cells expressing markers for the early-born cell types, RGCs, ACs, and HZs, were significantly increased in E12.5 *Pten-cko* retinas (Figure 4A, left two columns). There was also an enhanced development of Recoverin-positive PRs (Figure 4A, centre column) or PKCα-positive BP cells (Figure 4A, right first column) in E16.5 or P7 *Pten-cko* retinas, respectively. Furthermore, this interesting developmental acceleration in *Pten-cko* retinas was also observed in MG cells. In contrast to results obtained at P8, when the numbers of MGs and MG precursor cells in *Pten-cko* retinas were decreased (Figure 3L), at P4, more glutamine synthase

(GS)-positive mature MG cells were detected in *Pten-cko* retinas than in the *Pax6-aCre* retina (Figure 4A, second right column).

Because pAkt immunoreactivity was strongly enriched in post-mitotic neurons, but less in RPCs (Figure 1A), the hyperactivation of Akt upon *Pten* deletion might result in the accelerated neuronal differentiation of RPCs by facilitating the expression of neuronal markers in the cells (Figure 4A and B). In support of this, staining for the neuron-specific marker Tuj1 (class III β-tubulin) showed that not only the number of post-mitotic neurons in E12.5 *Pten-cko* retinas, but also the number of EGFP-positive RPCs, which are positive for Tuj1 neuronal marker, was also increased in *Pten-cko* retinas, whereas EGFP-positive *Pax6-aCre* RPCs were virtually negative for this marker (Figure 4C and D). Taken together, these results suggest that accelerated neuronal development in the *Pten-cko* retina may be mediated by premature expression of neuronal genes in RPCs.

Reduced Notch signalling in Pten-cko retinas
Premature retinal neurogenesis and defective maintenance of RPCs and MGs, both of which are prominent phenotypes of the *Pten-cko* retina, have also been described as developmental consequences of impaired Notch (Jadhav *et al*, 2006; Yaron *et al*, 2006; Nelson *et al*, 2007). Supporting the correlation of Notch signalling in impaired RPC maintenance, the level of Hes1 (hairy/enhancer of split 1), which is known to be a key downstream target of the Notch (Ohtsuka *et al*, 1999), was significantly reduced in E14.5 *Pten-cko* retina (Figure 5A). Furthermore, Hes1 expression and pAkt positiv-
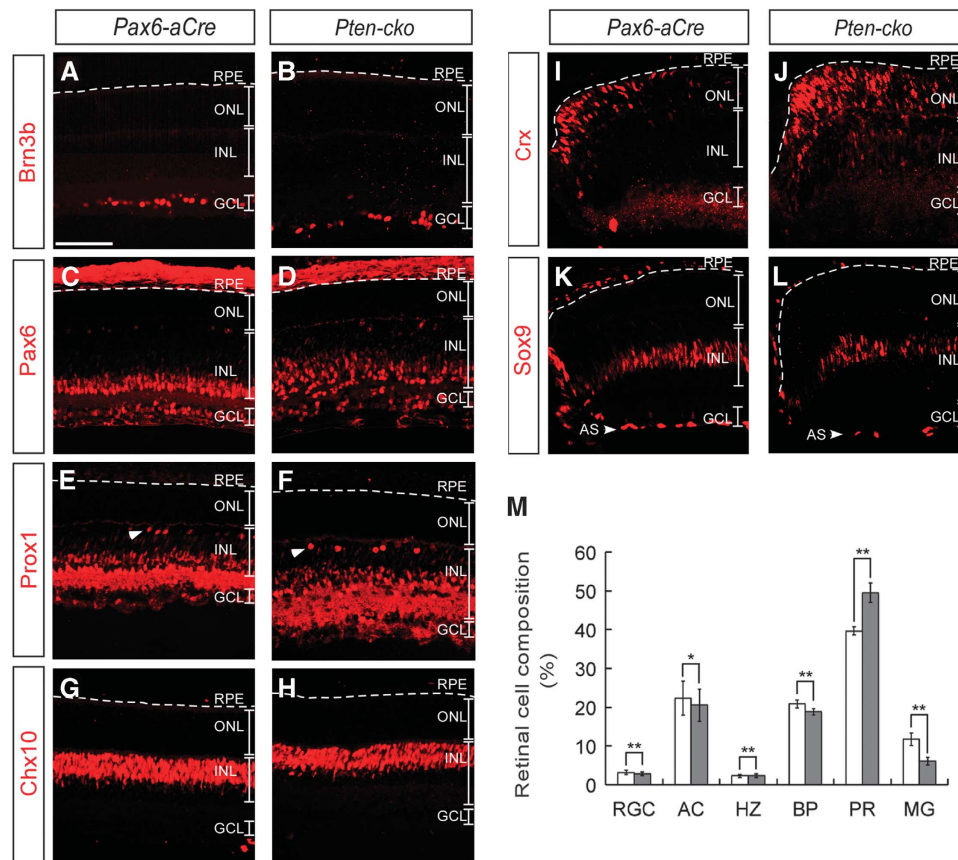
Figure 3 Decreased Müller glia numbers in *Pten-cko* retinas. The distribution of neuronal subtypes in P8 *Pax6-aCre* and *Pten-cko* mouse retinas was examined using the cell type-specific markers, Brn3b (**A**, **B**), for RGCs; Pax6 (**C**, **D**), for ACs; Prox1 (**E**, **F**), for HZs (arrowheads) and ACs; Chx10 (**G**, **H**), for BPs; Crx (**I**, **J**), for PRs; and Sox9 (**K**, **L**), for MGs. (**M**) Cell composition of *Pax6-aCre* (open bars) or *Pten-cko* (filled bars) littermate mouse retinas is shown. The numbers represent mean values obtained from four different retinal samples isolated from two independent litters. Error bars denote s.d. *P-value <0.01; **P-value <0.005. ONL, outer nuclear layer; INL, inner nuclear layer; GCL, ganglion cell layer. Scale bar, $50\,\mu m$.

ity were mutually exclusive in developing retina (Figure 5B), suggesting a negative relationship between these two attributes.

We, therefore, examined whether the expression of Notch1, which is major Notch isoform expressed in RPCs (Jadhav *et al*, 2006; Yaron *et al*, 2006; Nelson *et al*, 2007), and its ligand *delta-like 1* (*Dll1*) were changed in *Pten-cko* retinas. Both of *Notch1* and *Dll1* did not show significant changes in E14.5 *Pten-cko* retinas in comparison with those in *Pax6-aCre* littermate retinas, in contrast to remarkable reduction of *Hes1* in *Pten-cko* retinas (Supplementary Figure S6). These results, therefore, suggest the enhanced neurogenesis and premature depletion of RPCs in the *Pten-cko* retina were likely caused by reduced Notch intracellular signalling activity rather than transcriptional inhibition of Notch or Dll1.

Inefficient Notch transcription complex formation in Pten-cko retinas

Notch signal transduction is initiated by cleavage of Notch in the juxtamembrane domain by γ-secretase upon binding to Notch ligands; the resultant Notch intracellular domain (NICD) is released from the plasma membrane and enters the nucleus to activate target gene expression (Selkoe and Kopan, 2003). We, therefore, investigated whether the reduced Notch signalling in *Pten-cko* retina was caused by defective processing of Notch. The amount of full-length Notch1, Notch1 extracellular domain truncated form (N1-TM), and NICD in P0 *Pten-cko*

retinas, however, were largely unchanged in comparison with those of littermate *Pten-flox* retinas (Figure 5C). On the basis of these data, we conclude that the reduction in Hes1 expression in the *Pten-cko* retina was not caused by defective ligand-induced processing of Notch, but might have resulted from impaired NICD activity.

In the nucleus, NICD interacts with the transcription factors CBF1 (C promoter-binding factor 1)/RBP-Jκ (recombination signal-binding protein 1 for J-kappa) to activate target gene expression (Selkoe and Kopan, 2003). The NICD–CBF1 complex interacts with the scaffold protein Mastermind (MAM), which then recruits a transcription co-activator complex that contains the histone acetyl transferase (HAT) p300/CREB binding protein (CBP), to enhance transcription of target genes further (Fryer *et al*, 2002, 2004). To elucidate the regulatory roles of Pten and PI3K-Akt signalling in NICD activity, we examined the transcription complex formation among NICD, CBF1, and Mastermind-like 1 (MAML1) in P0 *Pten-flox* or *Pten-cko* mouse retinas by co-immunoprecipitation. The results indicate that the association of NICD with MAML1 as well as CBF1 was significantly reduced in the *Pten-cko* retinas (Figure 5D). The results, therefore, suggest that the reduced expression of Notch target Hes1 in Akt-hyperactive *Pten*-deficient RPCs might be correlated with the inefficient interaction of NICD with CBF1 transcription factor and MAML1 transcription co-activator.
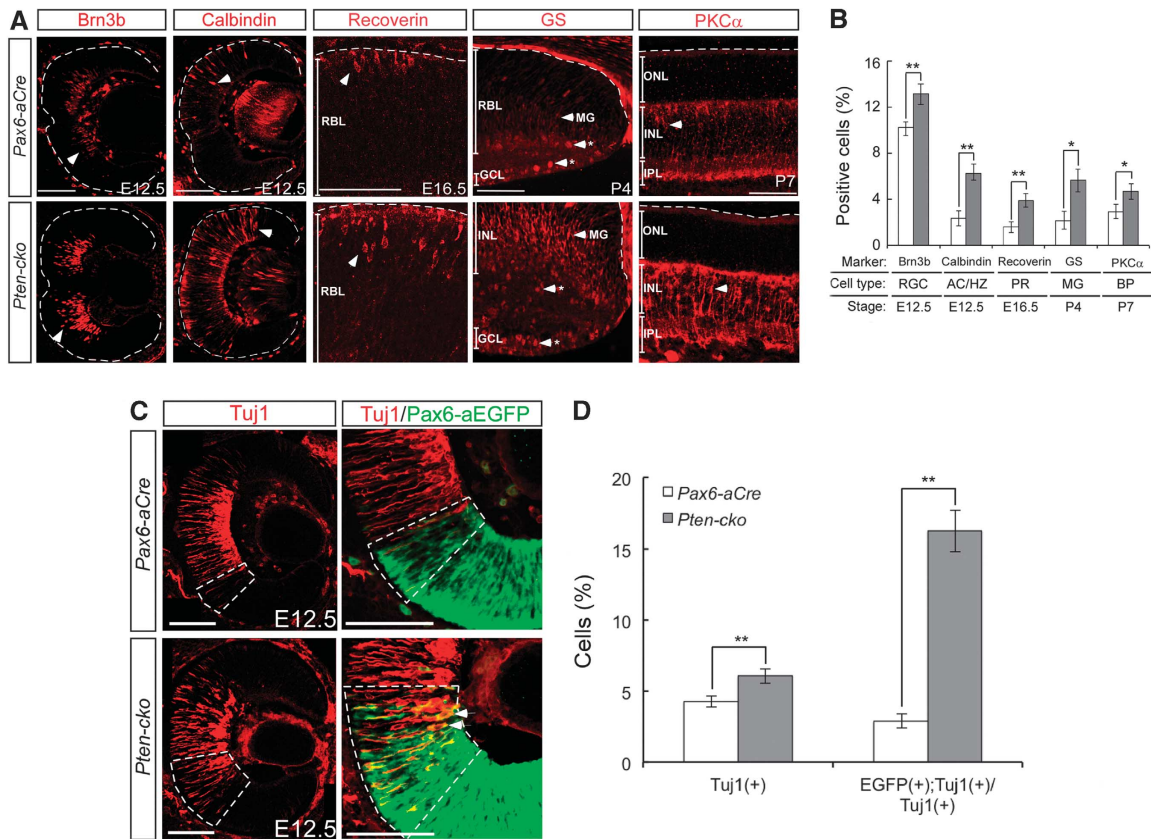
Figure 4 Accelerated development of *Pten-cko* retinas. (**A**) The distribution of mature forms of retinal neurons in developing *Pax6-aCre* and *Pten-cko* littermate mouse retinas was examined by immunostaining with antibodies against Brn3b, Calbindin, Recoverin, Glutamine synthase (GS), and Protein kinase C-α (PKCα). The time point examined for each cell type corresponds to the time at which the first signals are detectable. Asterisks (*) in GS staining images represent non-specifically stained cells. Scale bars, 50 μm. (**B**) Retinal cells expressing each marker were counted and mean numbers of positive cells per 1000 total cell counts are shown in *Y* axis. The values were obtained from six different immunostaining images of retinal sections, which were obtained from two independent litters. Error bars are s.d. *P-value < 0.01; **P-value < 0.005. (**C**) The distribution of post-mitotic neurons in E12.5 retinas was assessed by immunostaining with a neuron-specific class III β-tubulin antibody (Tuj1; red) and counterstaining with the RPC-specific markers Pax6-aEGFP (green). More Tuj1-positive post-mitotic neurons were EGFP positive in *Pten-cko* retinas (arrows) than in *Pax6-aCre* retinas, in which Tuj1 and EGFP positivity were mutually exclusive. Dashed boxes indicate areas where EGFP-positive RPCs and Tuj1-positive post-mitotic neurons intermingled. (**D**) The cells positive to Tuj1 or double positive to Tuj1 and Pax6-aEGFP were counted. The *Y* axis values are mean values obtained from five independent samples. Scale bars, 50 μm. Error bars are s.d. **P-value < 0.005.

We further found that hyperactivated Akt might be responsible for the inhibition of Notch transcription activity in the *Pten-cko* retinas. We reconstituted a cellular environment similar to that of the *Pten-cko* retina by co-expressing NICD with constitutively active Akt (Akt(CA)) in rat retinal progenitor R28 cells, and examined the effects of Akt activation on NICD transcription activity. We found that Akt(CA) markedly decreased NICD-induced *Hes1*-luciferase expression, whereas kinase inactive Akt[K179M] (Akt(KM)) slightly increased it (Supplementary Figure S7). We also found that the interaction between NICD and MAML1 was inhibited in R28 cells that co-express Akt(CA) (data not shown). These biochemical observations are consistent with our *in-vivo* observation that the expression of Hes1 was significantly reduced in the Akt-hyperactive *Pten-cko* retinas, where NICD transcription complex formation was inhibited (Figure 5).

Rescue of developmental defects in Pten-cko retina by ectopically expressed NICD

To determine whether reduced NICD transcription activator complexes is a prerequisite for the enhanced neurogenesis

and RPC depletion observed in the *Pten-cko* retina, we ectopically supplemented *Pten*-deficient RPCs with the Notch1 intracellular domain (NICD), an activated form of Notch1 (Struhl and Adachi, 1998; Selkoe and Kopan, 2003). To accomplish this, we bred *Pten-cko* mice with ROSA26-NICD-IRES-nEGFP (R26-NICD) mice, which overexpress NICD upon Cre-mediated excision of a loxP-flanked STOP fragment (Murtaugh *et al*, 2003). The number of pH3-positive mitotic nuclei, which were depleted in *Pten-cko* retinas, was greatly increased in the retinas of *R26-NICD;Pten-cko* mice (Figure 6A, top row column; quantified data are shown in Figure 6B). The ectopic expression of NICD also recovered the Sox2-positive RPC population in the retina (Figure 6A, middle row; Figure 6B). Furthermore, the MG population, which was reduced in the *Pten-cko* retina (Figure 3L), was significantly increased in the *R26-NICD;Pax6-aCre* retina (data not shown). In addition, the size of the rhodopsin-positive rPR population, which was increased in the retinas of *Pten-cko* mice, was normalized in the retinas of P4 *R26-NICD;Pten-cko* mice (Figure 6A, bottom row; Figure 6B). Taken together, these results indicate that both the premature depletion of RPC populations and the accelerated neuronal
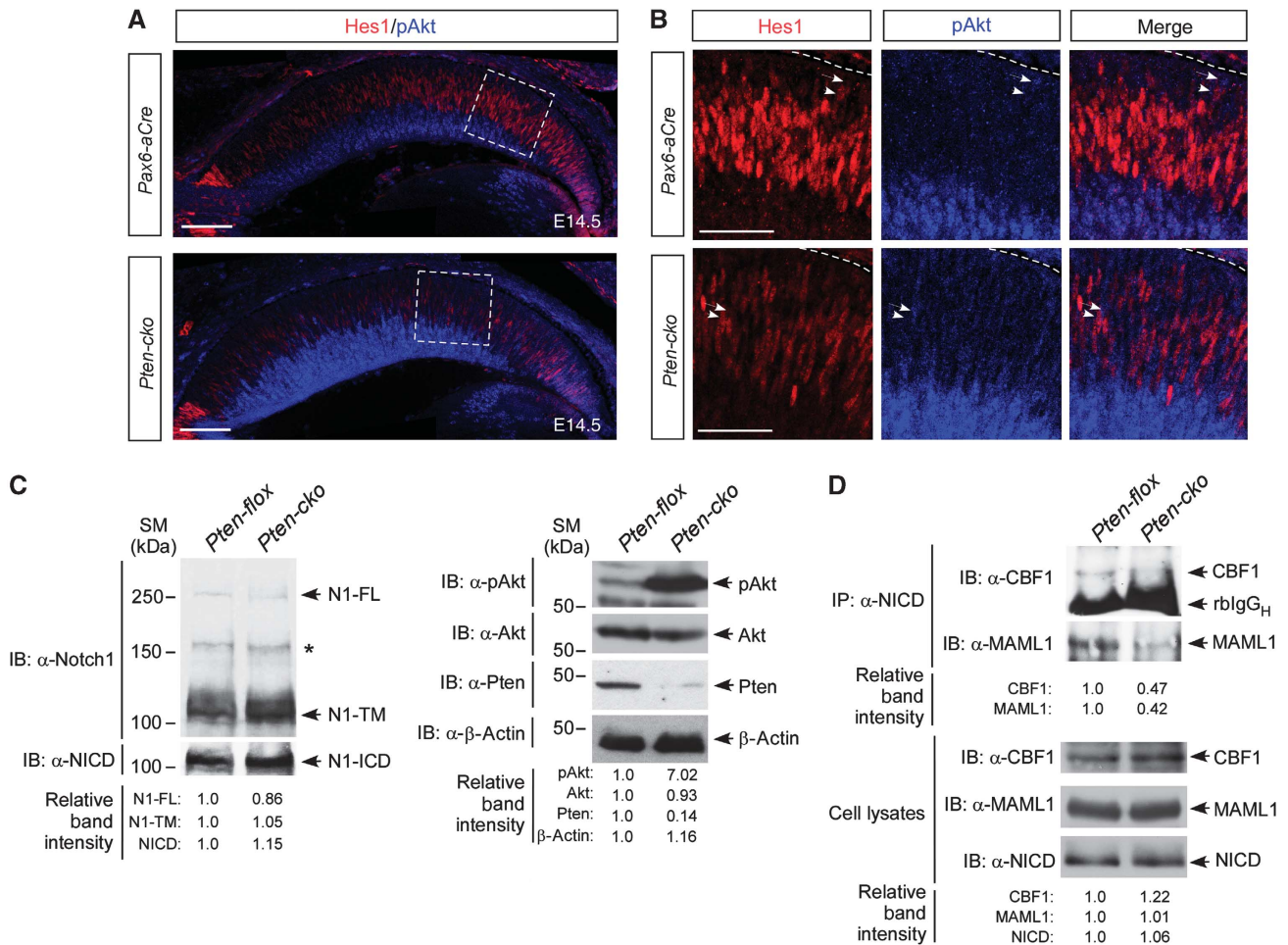
Figure 5 Reduced Notch signalling in *Pten-cko* mouse retina. (**A**) The expression of the Notch target Hes1 in E14.5 *Pax6-aCre* and *Pten-cko* mouse retina was examined by immunostaining with an anti-Hes1 antibody (red). Co-immunostaining with an anti-pAkt antibody (blue) revealed an inverse correlation between Hes1 expression and Akt activity. (**B**) Images are magnified versions of the boxed areas in (**A**). Arrows and arrowheads indicate pAkt- and Hes1-positive cells, respectively. (**C**) Neonatal (P0) retinal cell lysates (including 50 μg proteins/well) were analysed by western blotting using an anti-Notch1 antibody that recognizes the C-terminal region of mouse Notch1 (top panel of left column). The arrowheads in the top panel indicate full-length Notch1 (N1-FL); extracellular domain truncated Notch1 fragments with transmembrane domain and cytoplasmic domain (N1-TM). Asterisk (*) indicates non-specific proteins recognized by anti-Notch1 antibody. Notch1 intracellular domain (NICD) was detected by anti-NICD antibody to analyse γ-secretase-mediated cleavage of Notch1 (bottom panel of left column). The successful elimination of Pten and consequent hyperactivation of Akt in the retinal cells were confirmed by western blotting with anti-Pten, pAkt, and anti-Akt antibodies, respectively (right column). The amount of proteins in the lysates was normalized by the amount of β-actin. (**D**) The P0 *Pax6-aCre* and *Pten-cko* mouse retinal lysates (including 2 mg proteins) were subjected to immunoprecipitation with anti-NICD antibody (2 μg), and co-immunoprecipitated CBF1 and MAML1 proteins were detected by western blotting with anti-CBF1 or anti-MAML1 antibodies (see details in Materials and methods). rbIgG$_H$, rabbit immunoglobulin G heavy chain. The relative amounts of CBF1 and MAML1 in the cell lysates (including 50 μg proteins/well) were also examined by western blotting. Relative band intensity values in (**C**) and (**D**) were obtained by Image-J densitometry analysis program. Information for the antibodies is provided in Supplementary Table S2. Figure source data can be found in Supplementary data.

development in *Pten-cko* retina are due, at least in part, to impaired activation of the Notch signalling pathway.

Discussion

Premature depletion and hyperproliferation, similar to that observed here in *Pten*-deficient RPCs, have also been observed in *Pten*-deficient haematopoietic stem cells (HSCs; Yilmaz *et al*, 2006). Just as *Pten*-deficient RPCs were eventually depleted in the mature retina, *Pten*-deficient HSCs (except for leukaemia-initiating cells) gradually lose their potential for further division. Pten may act in this capacity by decelerating the rate of cell division and consequently reducing the number of cell divisions, thereby preventing cells from prematurely reaching their division limit. Consistent with this mode of action, the loss

of *Pten* results in overproduction of cells during both blood development and retinal development. Taken together, these results suggest that Pten plays a general role in preserving the stem cell populations necessary for extended production of mature cells in a variety of tissues, although it remains to be determined whether Notch is also an obligate downstream target of Pten in HSCs.

As summarized in Supplementary Table S1, activated Notch signalling contributes to RPC maintenance by preventing their premature exit from the cell cycle, whereas PI3K-Akt activation mainly facilitates RPC proliferation by accelerating cell-cycle progression. These two signalling events cooperate to develop retinoblastoma in *Pten-cko;R26-NICD* mice, of which RPCs kept both signalling pathways on hyperactive (Figure 6). In normal developing condition, however, these two signalling
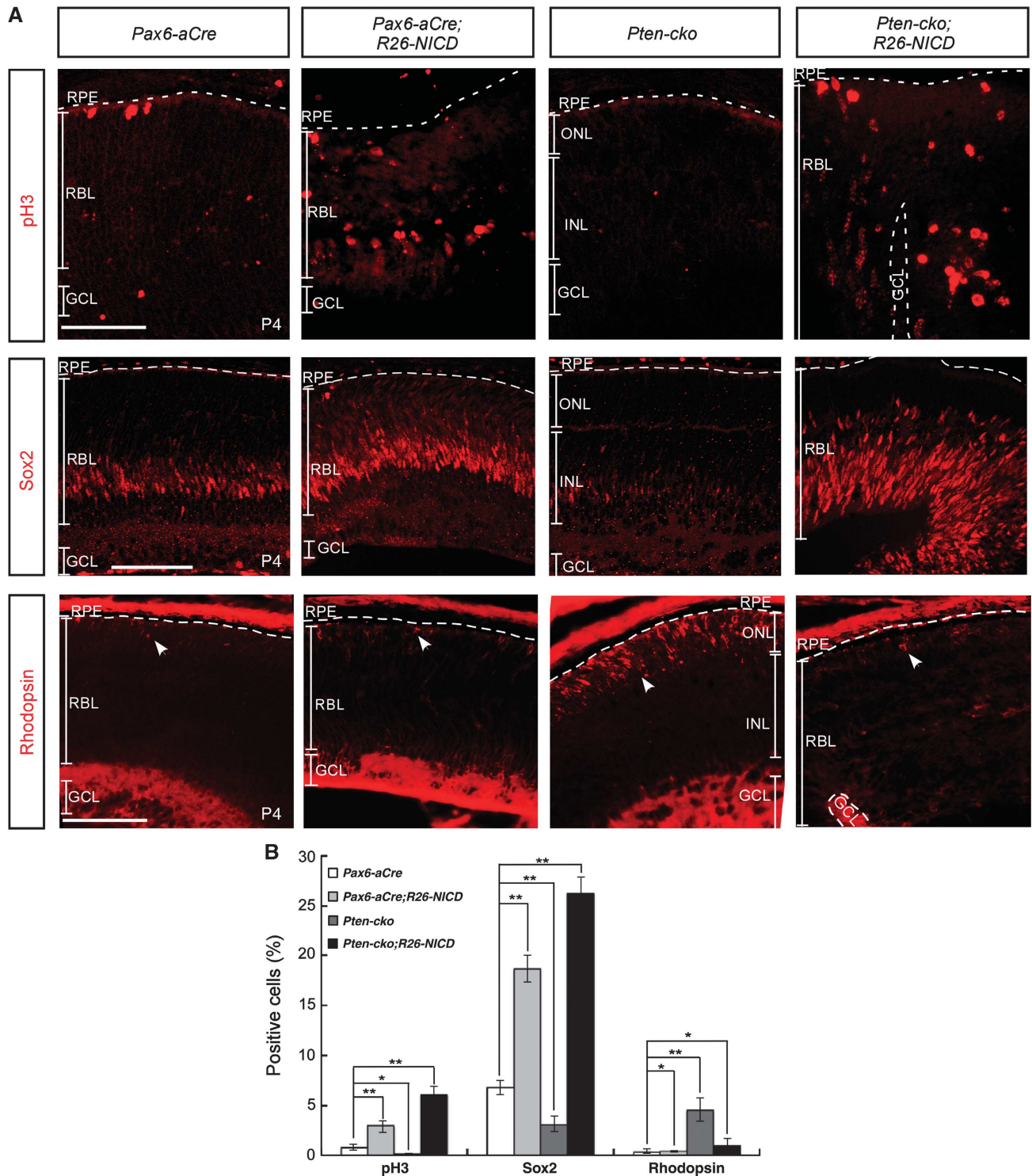
Figure 6 Ectopic NICD rescues developmental defects in *Pten-cko* retina. (**A**) The NICD was ectopically expressed in *Pax6-aCre* and *Pten-cko* mouse retinas upon Pax6-aCre-mediated excision of loxP-STOP-loxP gene cassette (Murtaugh *et al*, 2003). The decreased mitotic index, which was measured by counting the number of pH3-positive cells (top row), in P4 *Pten-cko* retina was recovered to a greater extent by ectopic expression of NICD than that of littermate *Pax6-aCre* retina. Sox2-positive RPCs (middle row), which were depleted in P4 *Pten-cko* retinas, also increased upon expression of NICD, whereas the number of prematurely differentiated Rhodopsin-expressing rPRs (bottom row, arrowheads) in *Pten-cko* retinas was decreased to normal levels. The dashed lines in the pictures denote the borders between retina and RPE. Scale bars, 50 μm. (**B**) Graph presents cells, which are positive to pH3, Sox2, or Rhodopsin in retinal sections of P4 *Pax6-aCre, Pax6-aCre;R26-NICD, Pten-cko*, or *Pten-cko;R26-NICD* littermate mice, including the images shown in (**A**). The values are averages in five different images obtained from three independent litters. Error bars are s.d. *P-value <0.005; **P-value <0.001 (Student's *t*-test). *P*-values for each marker obtained by one-way ANOVA test were <0.005 (results not shown).
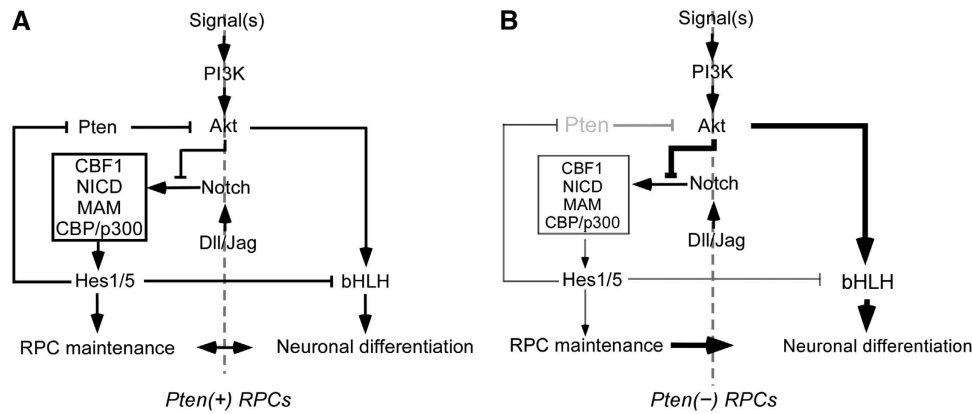
Figure 7 Pten plays a pivotal role in retinal neurogenesis by supporting temporal activation of Notch signalling in RPC. Pten supports Notch signalling by negatively regulating Akt that inactivates NICD transcription complex formation. The accumulated Notch transcription activator complex composed of CBF1, NICD, MAM, and CBP/p300 then induces the expression of downstream target genes including transcription repressor Hes1, one of which downstream target is Pten, to prevent RPCs from prematurely differentiating. As a result of Hes1-induced repression of Pten, Akt is reactivated to turn the Notch-induced transcriptions off, and consequently RPCs start to differentiate. Upon the disassembly of Notch transcription activator complex, Hes1 cannot be accumulated to repress Pten expression, and re-expressed Pten start to inhibit Akt. This feedback regulation loop coordinates retinal neurogenesis and RPC maintenance (**A**). In *Pten*-deficient RPCs, this feedback loop is broken. Consequently, the NICD fails to form transcription activator complex that is necessary for RPC maintenance (**B**).

events conflict with each other, especially when it comes to determining the fates of two daughter cells asymmetrically. Activated Notch signalling prevents daughter cells either from re-entering the next cell cycle prematurely or from exiting the cell cycle prematurely; therefore, RPC division speed is significantly retarded as observed in the *Pax6-aCre;R26-NICD* embryonic retina (data not shown). This results in the prolonged maintenance of RPCs in *Pax6-aCre;R26-NICD* mice, a majority of which continued to be capable of dividing during the postnatal period (Figure 6). In contrast, activated Akt in the *Pten-cko* retina interferes with the Notch-induced preservation of RPC fate by inhibiting Notch transcription activator complex formation (Figure 5D). Impeded Notch signalling, thus, fails to support the preservation of progenitor characteristics in daughter cells during asymmetric cell division, and cannot prevent these cells from differentiating prematurely (Figure 4). Therefore, Pten supports Notch signalling by negatively regulating Akt activity, and consequently prevent premature depletion of RPCs.

However, this protection of Notch by Pten might be only temporary, owing to feedback inhibition of *Pten* expression by the Notch pathway (Palomero *et al*, 2007). Once the Notch target Hes1 has accumulated sufficiently to maintain progenitor fate, it initiates a negative feedback loop by inhibiting expression of *Pten* (Palomero *et al*, 2007); this consequently restores the negative effects of Akt on Notch. Hes1-induced *Pten* repression is then also released, and Pten starts to reaccumulate until it reaches a level sufficient to inhibit Akt again (summarized in Figure 7A). The repeated operation of this feedback circuitry generates neurons and also maintains RPCs through the asymmetric acquisition of fates upon RPC division. If one of these key components is missing, the feedback loop cannot properly return to its starting point. In the *Pten-cko* retina, post-mitotic neurons therefore continue to accumulate due to a failure to maintain RPC fate (summarized in Figure 7B).

Previous studies have proposed that the repression of Notch transcriptional activity by PI3K-Akt signalling has been proposed to result from the cytoplasmic retention of

NICD (Baek *et al*, 2007; Song *et al*, 2008). However, it is unclear for significant changes in the nuclear-cytoplasmic distribution of NICD in *Pten-cko* mouse retinas (data not shown). Instead, we found that the Akt-induced inhibition of NICD activity likely resulted from interference with Notch-induced transcription activator complex formation with CBF1 and MAML1 (Figure 5D). It has been proposed that the phosphorylation-dependent regulation of NICD involves in disassembly of NICD transcription complex by facilitating NICD ubiquitination (Fryer *et al*, 2004; Chiang *et al*, 2006). NICD has no conserved Akt phosphorylation target sequences, however, the possibility that Akt interferes with NICD transcription complex formation by inducing NICD phosphorylation cannot be excluded.

The opposing roles of PI3K and Pten in controlling retinal neurogenesis that we describe in the mouse are consistent with previously reported effects on the movement of the morphogenetic furrow during *Drosophila* retinal neurogenesis (Gao *et al*, 2000; Bateman and McNeill, 2004). Just as the activated PI3K-Akt signalling pathway in *Pten-cko* mice stimulated retinal neurogenesis, activation of Akt by mosaic expression of the PI3K catalytic subunit *dp110*, or by *dPten* inactivation in *Drosophila* eye imaginal discs propels the neurogenic wave forward to encompass neighbouring wild-type cells (Bateman and McNeill, 2004). Insulin was shown to stimulate *Drosophila* retinal neurogenesis by activating the PI3K-Akt signalling pathway, which then targets the downstream effecter mTOR (Bateman and McNeill, 2004). However, the roles of insulin and mTOR as upstream and downstream components, respectively, of PI3K-Akt signalling in mouse retinal neurogenesis have not yet been clarified.

In this study, we investigated the role of the PI3K-Akt signalling pathway as an intracellular neurogenic signalling hub in RPCs. We found that Notch signalling is one such signal that could be integrated into the PI3K-Akt signalling pathway in RPCs through a feedback regulation loop. Although the PI3K-Akt signalling pathway and its negative

regulator Pten played essential roles in determining the fate of RPCs through crosstalk with Notch signalling, there are likely to be additional upstream as well as downstream factors that interact with the PI3K-Akt signalling cascade to influence retinal neurogenesis, including Shh (Riobo *et al*, 2006; Peltier *et al*, 2007), Wnt (Peng *et al*, 2004; Wolf *et al*, 2008), FGF (Fischer *et al*, 2002; Fischer, 2005), and IGF (Fischer, 2005). Downstream as well as upstream events that transduce the evolutionarily conserved neurogenic PI3K-Akt signalling cascades in the mouse retina, therefore, warrant further investigation.

Materials and methods

Mice
Pten-flox mice were bred with *Pax6-aCre* mice to generate *Pten-cko* mice (Marquardt *et al*, 2001; Suzuki *et al*, 2001). The distribution of cells underwent Cre-mediated recombination in *Pax6-aCre* and *Pten-cko* retinas was traced by breeding these mice with R26R-lacZ mice and assessing Cre-dependent R26-lacZ expression by X-gal staining (Soriano, 1999). The rescue of retinal abnormalities in *Pten-cko* mice by NICD was examined by breeding *Pax6-aCre* and *Pten-cko* mice with R26-NICD mice (Murtaugh *et al*, 2003).

Immunohistochemistry
After anaesthetizing pregnant mice by intraperitoneal injection of tribromoethanol (Avertin), embryos were isolated and fixed in a 4% PFA/PBS solution. Anaesthetized postnatal mice were perfused with a 4% PFA/PBS solution to fix the tissues. Embryos or eyes isolated from the mice were further fixed with 4% PFA/PBS in 4°C for 2 h, and then incubated in a 20% sucrose/PBS solution at 4°C for 16 h before embedding in OCT medium and freezing on dry ice. Sections (10–14 μm; horizontal axis) of frozen tissues on slides or transfected cells grown on coverslips were blocked with 5% normal donkey serum and 5% normal goat serum in PBS/1% Triton X-100 prior to incubating with appropriate primary antibodies (Supplementary Table S2) at 4°C for 16 h. The samples were then stained with Alexa488-, Cy3-, or Cy5-conjugated secondary antibodies, and subsequently analysed by confocal microscopy (Zeiss LSM510, LSM710, and Olympus FV1000). The cells stained with each antibody were counted, and statistical significance of values was determined by Student's *t*-test or analyses of variance (ANOVA) test.

BrdU labelling of proliferating cells or CldU/IdU double labelling to detect the re-entry of cell cycle
The pregnant or postnatal mice were injected with 5-bromo-2′-deoxyuridine (BrdU; 30 mg/kg) into their peritoneal cavity at 3 h prior to the isolation of embryos or eyes. For the double labelling with CldU and IdU, the mice were injected with 5-chloro-2′-deoxyuridine (CldU; 30 mg/kg) at 16 h before injecting with 5-iodo-2′-deoxyuridine (IdU; 30 mg/kg) followed by incubation for 3 h. The isolated samples were fixed in 4% paraformaldehyde (PFA)/phosphate-buffered saline (PBS) at 4°C for 16 h, and incubated in 20% sucrose/PBS for another 16 h prior to embedding into the OCT freezing medium. The sections of the frozen tissues were further fixed in 4% PFA/PBS for 5 min, and washed with PBS three times for the subsequent treatment with 2N HCl for 30 min. The samples were then neutralized their pH by immersing in 0.1 M borate buffer (pH 8.0) for 5 min three times, and then were subjected to the regular immunohistochemistry procedures described in below.

X-gal staining
Eyes isolated from mice that carried the R26R-lacZ allele were fixed with 4% PFA/PBS on ice for 30 min, and then incubated in 20% sucrose/PBS at 4°C until they sunk to the bottom of the solution. OTC-embedded frozen samples were sectioned onto slides (16-μm-thick slices). Slides were then washed three times with cold PBS, and incubated in X-gal staining solution for 16 h at 37°C as reported previously (Mui *et al*, 2005).

In-situ RNA hybridization
Mice were perfused with 4% PFA in DEPC-treated PBS, and the embryonic heads or isolated postnatal mouse eyes were further fixed in the same solution for 16 h at 4°C. The tissues were then embedded in OCT medium after incubating in 20% sucrose/PBS for 16 h at 4°C. Frozen tissues sections (16 μm) were analysed by *in-situ* RNA hybridization as described previously with some modification (Mehler, 2002). Expression of the mRNA of interest in the retina was detected by hybridizing the sections with digoxigenin-11-(2′-deoxy-uridine-5′)-triphosphate (DIG-11-dUTP)-labelled RNA prepared from the corresponding cDNAs, and then assessing the activity of alkaline phosphatase conjugated to the labelled RNA-bound anti-digoxigenin (DIG) antibody.

Cell culture, transfection, and luciferase assay
Rat retinal progenitor R28 cells were maintained in Dulbecco's Modified Eagle Medium (DMEM) with 10% fetal bovine serum (FBS). Cells were transfected with Lipofectamine Plus (Invitrogen) as recommended by the manufacturer. For reporter assays, a CBF1 reporter DNA construct containing a *Hes1* promoter sequence fused to the firefly luciferase cDNA was co-transfected with DNA constructs of interest (Jarriault *et al*, 1995). Cells were also co-transfected with pSV-β-galactosidase to normalize luciferase activity to the transfection efficiency in each sample. After 24 h, extracts from transfected cells were prepared and processed using the Luciferase Assay System (Promega) and luciferase activity was measured in a Microlumat LB 96P Luminometer (Berthold).

Co-immunoprecipitation
Neonatal (P0) *Pten-flox* or *Pten-cko* mouse eyes were isolated, and their lenses were removed. The retinas were then smoothly squeezed out from the enucleated eyes, and were immediately kept in frozen until confirming their genotypes. Littermate mouse retinas with same genotypes were then collected for the lysis in a buffer containing 10 mM Tris–HCl (pH 7.4), 200 mM NaCl, 1% Triton X-100, and 1% NP-40. Cell lysates were centrifuged at 12 000 *g* for 10 min, and the resulting supernatant was incubated with appropriate antibodies at 4°C for 16 h. Protein A-sepharose was then added to the samples, and the protein A-sepharose bead/immune complexes were washed five times with lysis buffer prior to western blot analyses to detect co-immunoprecipitated proteins.

Statistical analysis
Data obtained from statistical analyses are presented as the mean ± s.d. Student's *t*-test was used to determine the significant difference between two groups and one-way ANOVA was used for determining the significant difference among multiple groups. We considered the *P*-value < 0.05 as statistically significant results.

Supplementary data
Supplementary data are available at *The EMBO Journal* Online (http://www.embojournal.org).

Conflict of interest

The authors declare that they have no conflict of interest.

References

Agathocleous M, Harris WA (2009) From progenitors to differentiated cells in the vertebrate retina. *Annu Rev Cell Dev Biol* **25:** 45–69

Alessi DR, Andjelkovic M, Caudwell B, Cron P, Morrice N, Cohen P, Hemmings BA (1996) Mechanism of activation of protein kinase B by insulin and IGF-1. *EMBO J* **15:** 6541–6551

Baek SH, Kim MY, Mo JS, Ann EJ, Lee KS, Park JH, Kim JY, Seo MS, Choi EJ, Park HS (2007) Zinc-induced downregulation of Notch signaling is associated with cytoplasmic retention of Notch1-IC and RBP-Jk via PI3k-Akt signaling pathway. *Cancer Lett* **255:** 117–126

Bateman JM, McNeill H (2004) Temporal control of differentiation by the insulin receptor/tor pathway in Drosophila. *Cell* **119:** 87–96

Cantley LC (2002) The phosphoinositide 3-kinase pathway. *Science* **296:** 1655–1657

Cayouette M, Barres BA, Raff M (2003) Importance of intrinsic mechanisms in cell fate decisions in the developing rat retina. *Neuron* **40:** 897–904

Cepko CL, Austin CP, Yang X, Alexiades M, Ezzeddine D (1996) Cell fate determination in the vertebrate retina. *Proc Natl Acad Sci USA* **93:** 589–595

Chen CM, Cepko CL (2000) Expression of Chx10 and Chx10-1 in the developing chicken retina. *Mech Dev* **90:** 293–297

Chiang MY, Xu ML, Histen G, Shestova O, Roy M, Nam Y, Blacklow SC, Sacks DB, Pear WS, Aster JC (2006) Identification of a conserved negative regulatory sequence that influences the leukemogenic activity of NOTCH1. *Mol Cell Biol* **26:** 6261–6271

Chiaradonna F, Balestrieri C, Gaglio D, Vanoni M (2008) RAS and PKA pathways in cancer: new insight from transcriptional analysis. *Front Biosci* **13:** 5257–5278

Cho SH, Cepko CL (2006) Wnt2b/beta-catenin-mediated canonical Wnt signaling determines the peripheral fates of the chick eye. *Development* **133:** 3167–3177

Edlund T, Jessell TM (1999) Progression from extrinsic to intrinsic signaling in cell fate specification: a view from the nervous system. *Cell* **96:** 211–224

Elshatory Y, Deng M, Xie X, Gan L (2007) Expression of the LIM-homeodomain protein Isl1 in the developing and mature mouse retina. *J Comp Neurol* **503:** 182–197

Engelman JA, Luo J, Cantley LC (2006) The evolution of phosphatidylinositol 3-kinases as regulators of growth and metabolism. *Nat Rev Genet* **7:** 606–619

Fischer AJ (2005) Neural regeneration in the chick retina. *Prog Ret Eye Res* **24:** 161–182

Fischer AJ, Dierks BD, Reh TA (2002) Exogenous growth factors induce the production of ganglion cells at the retinal margin. *Development* **129:** 2283–2291

Fryer CJ, Lamar E, Turbachova I, Kintner C, Jones KA (2002) Mastermind mediates chromatin-specific transcription and turnover of the Notch enhancer complex. *Genes Dev* **16:** 1397–1411

Fryer CJ, White JB, Jones KA (2004) Mastermind recruits CycC:CDK8 to phosphorylate the Notch ICD and coordinate activation with turnover. *Mol Cell* **16:** 509–520

Furukawa T, Mukherjee S, Bao ZZ, Morrow EM, Cepko CL (2000) rax, Hes1, and notch1 promote the formation of Muller glia by postnatal retinal progenitor cells. *Neuron* **26:** 383–394

Gao X, Neufeld TP, Pan D (2000) Drosophila PTEN regulates cell growth and proliferation through PI3K-dependent and -independent pathways. *Dev Biol* **221:** 404–418

Gotz M, Huttner WB (2005) The cell biology of neurogenesis. *Nat Rev Neurosci* **6:** 777–788

Gould CM, Newton AC (2008) The life and death of protein kinase C. *Curr Drug Targets* **9:** 614–625

Harris WA (1997) Cellular diversification in the vertebrate retina. *Curr Opin Genet Dev* **7:** 651–658

Hui L, Bakiri L, Stepniak E, Wagner EF (2007) p38alpha: a suppressor of cell proliferation and tumorigenesis. *Cell Cycle* **6:** 2429–2433

Jadhav AP, Mason HA, Cepko CL (2006) Notch 1 inhibits photoreceptor production in the developing mammalian retina. *Development* **133:** 913–923

Jarriault S, Brou C, Logeat F, Schroeter EH, Kopan R, Israel A (1995) Signalling downstream of activated mammalian Notch. *Nature* **377:** 355–358

Kim J, Wu HH, Lander AD, Lyons KM, Matzuk MM, Calof AL (2005) GDF11 controls the timing of progenitor cell competence in developing retina. *Science* **308:** 1927–1930

Kim JW, Kang KH, Burrola P, Mak TW, Lemke G (2008) Retinal degeneration triggered by inactivation of PTEN in the retinal pigment epithelium. *Genes Dev* **22:** 3147–3157

Lamba D, Karl M, Reh T (2008) Neural regeneration and cell replacement: a view from the eye. *Cell Stem Cell* **2:** 538–549

Liu H, Xu S, Wang Y, Mazerolle C, Thurig S, Coles BL, Ren JC, Taketo MM, van der Kooy D, Wallace VA (2007) Ciliary margin transdifferentiation from neural retina is controlled by canonical Wnt signaling. *Dev Biol* **308:** 54–67

Livesey FJ, Cepko CL (2001) Vertebrate neural cell-fate determination: lessons from the retina. *Nat Rev Neurosci* **2:** 109–118

Marquardt T, Ashery-Padan R, Andrejewski N, Scardigli R, Guillemot F, Gruss P (2001) Pax6 is required for the multipotent state of retinal progenitor cells. *Cell* **105:** 43–55

Mehler MF (2002) Mechanisms regulating lineage diversity during mammalian cerebral cortical neurogenesis and gliogenesis. *Results Probl Cell Differ* **39:** 27–52

Mui SH, Kim JW, Lemke G, Bertuzzi S (2005) Vax genes ventralize the embryonic eye. *Genes Dev* **19:** 1249–1259

Murtaugh LC, Stanger BZ, Kwan KM, Melton DA (2003) Notch signaling controls multiple steps of pancreatic differentiation. *Proc Natl Acad Sci USA* **100:** 14920–14925

Nelson BR, Hartman BH, Georgi SA, Lan MS, Reh TA (2007) Transient inactivation of Notch signaling synchronizes differentiation of neural progenitor cells. *Dev Biol* **304:** 479–498

Ohtsuka T, Ishibashi M, Gradwohl G, Nakanishi S, Guillemot F, Kageyama R (1999) Hes1 and Hes5 as notch effectors in mammalian neuronal differentiation. *EMBO J* **18:** 2196–2207

Palomero T, Sulis ML, Cortina M, Real PJ, Barnes K, Ciofani M, Caparros E, Buteau J, Brown K, Perkins SL, Bhagat G, Agarwal AM, Basso G, Castillo M, Nagase S, Cordon-Cardo C, Parsons R, Zuniga-Pflucker JC, Dominguez M, Ferrando AA (2007) Mutational loss of PTEN induces resistance to NOTCH1 inhibition in T-cell leukemia. *Nat Med* **13:** 1203–1210

Park KK, Liu K, Hu Y, Smith PD, Wang C, Cai B, Xu B, Connolly L, Kramvis I, Sahin M, He Z (2008) Promoting axon regeneration in the adult CNS by modulation of the PTEN/mTOR pathway. *Science* **322:** 963–966

Peltier J, O'Neill A, Schaffer DV (2007) PI3K/Akt and CREB regulate adult neural hippocampal progenitor proliferation and differentiation. *Dev Neurobiol* **67:** 1348–1361

Peng Y, Jiang BH, Yang PH, Cao Z, Shi X, Lin MC, He ML, Kung HF (2004) Phosphatidylinositol 3-kinase signaling is involved in neurogenesis during Xenopus embryonic development. *J Biol Chem* **279:** 28509–28514

Raff M (2006) The mystery of intracellular developmental programmes and timers. *Biochem Soc Transac* **34:** 663–670

Raman M, Chen W, Cobb MH (2007) Differential regulation and properties of MAPKs. *Oncogene* **26:** 3100–3112

Riobo NA, Lu K, Emerson Jr CP (2006) Hedgehog signal transduction: signal integration and cross talk in development and cancer. *Cell Cycle* **5:** 1612–1615

Salmena L, Carracedo A, Pandolfi PP (2008) Tenets of PTEN tumor suppression. *Cell* **133:** 403–414

Selkoe D, Kopan R (2003) Notch and Presenilin: regulated intramembrane proteolysis links development and degeneration. *Ann Rev Neurosci* **26:** 565–597

Song J, Park S, Kim M, Shin I (2008) Down-regulation of Notch-dependent transcription by Akt *in vitro*. *FEBS Lett* **582:** 1693–1699

Soriano P (1999) Generalized lacZ expression with the ROSA26 Cre reporter strain. *Nat Genet* **21:** 70–71

Stork PJ, Schmitt JM (2002) Crosstalk between cAMP and MAP kinase signaling in the regulation of cell proliferation. *Trends Cell Biol* **12:** 258–266

Struhl G, Adachi A (1998) Nuclear access and action of notch *in vivo*. *Cell* **93:** 649–660

Suzuki A, Yamaguchi MT, Ohteki T, Sasaki T, Kaisho T, Kimura Y, Yoshida R, Wakeham A, Higuchi T, Fukumoto M, Tsubata T, Ohashi PS, Koyasu S, Penninger JM, Nakano T, Mak TW (2001) T cell-specific loss of Pten leads to defects in central and peripheral tolerance. *Immunity* **14:** 523–534

Turner DL, Snyder EY, Cepko CL (1990) Lineage-independent determination of cell type in the embryonic mouse retina. *Neuron* **4:** 833–845

Wang YP, Dakubo G, Howley P, Campsall KD, Mazarolle CJ, Shiga SA, Lewis PM, McMahon AP, Wallace VA (2002) Development of normal retinal organization depends on Sonic hedgehog signaling from ganglion cells. *Nat Neurosci* **5:** 831–832

Wolf AM, Lyuksyutova AI, Fenstermaker AG, Shafer B, Lo CG, Zou Y (2008) Phosphatidylinositol-3-kinase-atypical protein kinase C signaling is required for Wnt attraction and anterior-posterior axon guidance. *J Neurosci* **28:** 3456–3467

Yaron O, Farhy C, Marquardt T, Applebury M, Ashery-Padan R (2006) Notch1 functions to suppress cone-photoreceptor fate specification in the developing mouse retina. *Development* **133:** 1367–1378

Yilmaz OH, Valdez R, Theisen BK, Guo W, Ferguson DO, Wu H, Morrison SJ (2006) Pten dependence distinguishes haematopoietic stem cells from leukaemia-initiating cells. *Nature* **441:** 475–482

Zhong W, Chia W (2008) Neurogenesis and asymmetric cell division. *Curr Opin Neurobiol* **18:** 4–11